Revised theory of the magnetic surface anisotropy of impurities in metallic mesoscopic samples

O. Újsághy,[1] L. Szunyogh,[2] and A. Zawadowski[1,2,3]

[1]*Institute of Physics, Budapest University of Technology and Economics and Research Group Physics of Condensed Matter,*
Hungarian Academy of Sciences, H-1521 Budapest, Hungary
[2]*Department of Theoretical Physics, Budapest University of Technology and Economics, H-1521 Budapest, Hungary*
[3]*Research Institute for Solid State Physics, P.O.Box 49, H-1525 Budapest, Hungary*

In several experiments, the magnitude of the contribution of magnetic impurities to the Kondo resistivity shows size dependence in mesoscopic samples. It was suggested ten years ago that magnetic surface anisotropy can be responsible for the size dependence in cases where there is strong spin-orbit interaction in the metallic host. The anisotropy energy has the form $\Delta E = K_d(\mathbf{nS})^2$, where $\mathbf{n}$ is the vector perpendicular to the plane surface, $\mathbf{S}$ is the spin of the magnetic impurity, and $K_d > 0$ is inversely proportional to distance d measured from the surface. It has been realized that in the tedious calculation, an unjustified approximation was applied for the hybridizations of the host atom orbitals with the conduction electrons, which depend on the position of the host atoms. That is, the momenta of the electrons were replaced by the Fermi momentum k_F. That is reinvestigated by considering the k-dependence, which leads to singular energy integrals. Contrary to the previous result, K_d is oscillating like $\sin(2k_Fd)$ and the distance dependence is similar to $1/d^3$ in the asymptotic region. As the anisotropy is oscillating, for integer spin the ground state is either a singlet or a doublet depending on distance d, but in the case of the doublet there is no direct electron induced transition between those two states at zero temperature. Furthermore, for half-integer $(S > 1/2)$ spin it is always a doublet with direct transition only in half of the cases.

I. INTRODUCTION

There is substantial experimental evidence that the amplitude of the Kondo effect due to magnetic impurities in metallic samples of limited size is reduced[1,2] but with unchanged Kondo temperature. This indicates that not all of the impurities contribute in the same way. There were early speculations that this reduction appears when the sample size is comparable to the Kondo screening cloud. This is incorrect as the Kondo coupling is local and the only relevant energy scale to be compared with the Kondo temperature is the level spacing of the conduction electrons which is, e.g., zero for semi-infinite samples. Later, it was suggested[3] that a magnetic surface anisotropy can develop due to the spin-orbit interaction in the host metal, which has the form

$$H = K_d(S_z)^2, \tag{1}$$

where the constant K_d depends on the distance measured from the surface of the sample and S_z is the component of the impurity spin perpendicular to the surface (see Fig. 1). In those papers[2–4] it was stated that, surprisingly, K_d for large distances is always positive and decays with the first power of the distance. That result was not questioned in Ref. 5. Recently, one of the authors (Szunyogh) has called attention to an unjustified approximation in the previous lengthy calculation, which can be responsible for the very surprising results. That approximation was that in the hybridizations of the host atom orbitals with the conduction electrons which depend on the position of the host atoms [see Eqs. (3) and (9) of Ref. 4], the momenta of the electrons were replaced by the Fermi momentum k_F. That is not the case in the derivation of the Friedel oscillation.[6]

Meanwhile, great effort has been made to derive the surface anisotropy by using electronic structure calculations. First, Szunyogh and Gyorffy calculated the anisotropy in semi-infinite Au host for Fe impurities.[7] They found that K_d is an oscillating function of the distance d and the amplitude falls as $1/d^2$. That was a calculation of mean-field type and the discrepancy between those and the analytical ones was not surprising since, in the latter, the diagrams calculated are beyond the mean-field approximation. Recently, Szunyogh, *et al.*[8] have developed another model, where the spin-orbit interaction was placed on the d-level of the impurity instead of the host. They considered the Friedel oscillation in the density of states near the Fermi energy as due to the presence of the surface and the different d-orbitals of the impurity coupled differently to these oscillations, and that is realized in the oscillating anisotropy decaying as $1/d^2$. It is interesting to note that the Hartree-Fock mean-field approximation and the diagram beyond that play equal roles. We are also informed that very elaborate calculations by Szilva *et al.*[9] are in progress, where the spin-orbit interaction in the host is considered.

The relative importance of the spin-orbit interactions on the d-level and the host material must be very specific for which impurity atom and host metal are considered, and the
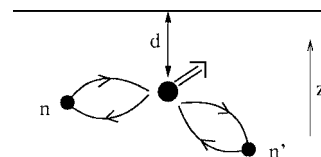

FIG. 1. The magnetic impurity at a distance d from the surface in a metallic host with homogeneously dispersed spin-orbit scatterers labeled by n.

final answer can be given only by detailed electronic structure calculations.

The present analytical calculation is focused on the oscillating behavior and the decay rate of the K_d function. All the results are obtained in the large distance asymptotic region, as the preasymptotic calculation would be even more difficult. The consequences of the oscillating behavior will be discussed at the end of the paper. The main goal is to present correct analytical result to be compared in the future with the numerical results, which may lead to the resolution of the present discrepancies. The comparison with the experiments is left for future work when the numerical calculation, by which the very relevant preasymptotic behavior is also achievable, is completed.

The paper is organized as follows. In Sec. II, we present the outline of the problem and call attention to the differences between the calculations here and those of the earlier works.[3,4] In Sec. III, the integrals with respect to the energies are performed, this is crucial in obtaining the correct form of the anisotropy. The consequences are analyzed in Sec. IV. Some of the matrix elements and further details of the calculations are presented in Appendixes A and B, respectively.

II. THE OUTLINE OF THE PROBLEM

The magnetic impurity scatters the electron in the $l=2$ orbital channel, and the spin-orbit scattering is also restricted to those.[3,4] As in Refs. 3 and 4, we start with the conduction electron propagator leaving and arriving at the impurity and in the meantime is scattered by one of the heavy host atoms due to strong spin-orbit scattering. Green's function has a simple form in the coordinate system where the impurity is in the origin and the scattering atoms is on the z axis at a position R_n, which is called the local system labeled by n. The Anderson model[10] is used for the scattering d-levels of the host atom and the spin-orbit scattering is assumed to happen on the d-level, and that determines the symmetry. Following Ref. 4 the conduction electron Green's function in first order of the spin-orbit coupling is

$$G_{km\sigma,k'm'\sigma'}(i\omega_n) = \frac{\delta_{kk'}\delta_{mm'}\delta_{\sigma\sigma'}}{i\omega_n - \varepsilon_k}$$

$$+ \sum_n \frac{1}{i\omega_n - \varepsilon_k} \frac{W_{kk'}(R_n)}{(i\omega_n - \omega_d)(i\omega_n - \omega_d)}$$

$$\times \frac{1}{i\omega_n - \varepsilon_{k'}}, \quad (2)$$

where now the k dependence in W and the ω dependence in the d-level Green's function are kept i.e., $G_d(i\omega_n)=1/(i\omega_n - \omega_d)$, where $\omega_d = \varepsilon_d - i\Delta$ and ε_d (measured from the Fermi level) and Δ are the energy and width of the d-level, respectively, and $-2 \leq m \leq 2$ for the conduction electrons.
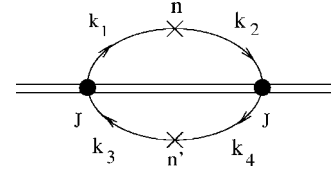
In Eq. (2), we now have

FIG. 2. The self-energy diagram for the impurity spin. The double line represents the spin, while the single one the conduction electrons. The solid circles stand for the exchange interaction and the crosses $\times$, labeled by n for the effective spin-orbit interaction on the orbital of the host atom at $\mathbf{R}_n$.

$$W_{kk'}(R_n)_{mm'\atop\sigma\sigma'}$$

$$= \lambda V^2 [B^+(k,k')\sigma^- + B^-(k,k')\sigma^+ + B^z(k,k')\sigma^z]_{mm'\sigma\sigma'},$$

$$(3)$$

which follows from a calculation similar to that in Ref. 4 and λ is the strength of the spin-orbit interaction. $B^\pm(k,k')$ and $B^z(k,k')$ are 5×5 matrices in the quantum number m, having the forms

$$B^+_{mm'}(k,k') = \sqrt{(3+m')(2-m')}\,v_m(k)v_{m'}(k')\delta_{m,m'+1},$$

$$(4a)$$

$$B^-_{mm'}(k,k') = \sqrt{(3-m')(2+m')}\,v_m(k)v_{m'}(k')\delta_{m,m'-1},$$

$$(4b)$$

$$B^z_{mm'(k,k')} = m\,v_m(k)v_{m'}(k')\delta_{m,m'},$$

$$(4c)$$

where the $v_m(k)$ matrix elements given in Appendix A are the same as in Eq. (13) of Ref. 4. These are combinations of oscillating functions $\sin(kR_n)$ and $\cos(kR_n)$ combined with powers like $(kR_n)^{-m-n}$ ($n=1,2,\ldots$).

The next step of the calculation is the rotation of the coordinate system from the n-local one to the one where the z axis is perpendicular to the surface. The angle between the z axis of the old (z_n) and the new (z) coordinate system is labeled by Θ_n. The calculation of the spin factor of the self-energy diagram (see Fig. 2) giving the anisotropy for the impurity spin is also similar to the original one [see Eqs. (21)–(25) of Ref. 4].

The average over the positions of the scattering atoms R_n and $R_{n'}$ must be performed for the whole volume of the sample, separately. For the sake of simplicity, the continuous limit is applied outside the impurity spin. As was shown in earlier works,[2–4] in order to get the dominant contribution, one of the n's is near the impurity and the other one experiences the existence of the surface at large distances.

The analytical part of the self-energy diagram (Fig. 2) is now, however, more complicated as the W's also depend on four different electronic momenta and the corresponding energies appear in the energy denominators of the electron

Green's functions. In this way, the prefactors also depend on the momenta, and that plays a crucial role in the following.

For the sake of simplicity, we consider the conduction electron band with constant density of states ρ_0 in the energy interval $-D < \varepsilon < D$, where ε is measured from the Fermi energy, and we will assume linear dispersion, i.e., the corresponding k values are $k = k_F + \varepsilon / v_F$, where v_F is the Fermi velocity.

As in a noble metal host such as Cu, Ag, or Au the d-band is below the Fermi energy, it does not give a new singularity in the energy integrals (see Sec. III); thus, we can replace the d-level propagator by a constant ϵ_0^{-1}.

Calculating the contribution of the diagram in Fig. 2, we applied Abrikosov's pseudofermion technique[11] for the spin. After performing the summation over the Matsubara frequencies, we get

$$\rho_0^4 \int_{-D}^{D} d\varepsilon_1 \int_{-D}^{D} d\varepsilon_2 \int_{-D}^{D} d\varepsilon_3 \int_{-D}^{D} d\varepsilon_4 \left\{ \frac{1}{\varepsilon_1 - \varepsilon_2} \frac{[1 - n_F(\varepsilon_1)]n_F(\varepsilon_3)}{\varepsilon_3 + \omega - \varepsilon_1} \frac{1}{\varepsilon_3 - \varepsilon_4} + (\varepsilon_1 \leftrightarrow \varepsilon_2) + (\varepsilon_3 \leftrightarrow \varepsilon_4) \right.$$

$$\left. + (\varepsilon_1 \leftrightarrow \varepsilon_2 \text{ and } \varepsilon_3 \leftrightarrow \varepsilon_4) \right\} \{ S^2 F_1(R_n, \theta_n, R_{n'}, \theta_{n'}; k_1, k_2, k_3, k_4) + S_z^2 F_2(R_n, \theta_n, R_{n'}, \theta_{n'}; k_1, k_2, k_3, k_4) \}, \tag{5}$$

where ω is the energy of the spin after analytical continuation and the F_1 and F_2 functions given in Appendix A are defined in the same way as in Ref. 4.

As that diagram contains two host atoms, averages have to be taken over n and n'. According to our simple model,[4] the anisotropy factor[3,4] reads as:

$$K = \frac{1}{a^6} \int d^3 R_n \int d^3 R_{n'} \rho_0^4 \int_{-D}^{D} d\varepsilon_1 \int_{-D}^{D} d\varepsilon_2 \int_{-D}^{D} d\varepsilon_3 \int_{-D}^{D} d\varepsilon_4 \left\{ \frac{1}{\varepsilon_1 - \varepsilon_2} \frac{[1 - n_F(\varepsilon_1)]n_F(\varepsilon_3)}{\varepsilon_3 + \omega - \varepsilon_1} \frac{1}{\varepsilon_3 - \varepsilon_4} + (\varepsilon_1 \leftrightarrow \varepsilon_2) + (\varepsilon_3 \leftrightarrow \varepsilon_4) \right.$$

$$\left. + (\varepsilon_1 \leftrightarrow \varepsilon_2 \text{ and } \varepsilon_3 \leftrightarrow \varepsilon_4) \right\} F_2(R_n, \theta_n, R_{n'}, \theta_{n'}; k_1, k_2, k_3, k_4), \tag{6}$$

where a^3 is the size of the volume per host atom.

By changing the order of the summation over the host atoms with the energy integrals, the former can be evaluated in a similar way as in Ref. 4.

Equation (29) of Ref. 4 now reads

$$K = \rho_0^4 \int_{-D}^{D} d\varepsilon_1 \int_{-D}^{D} d\varepsilon_2 \int_{-D}^{D} d\varepsilon_3 \int_{-D}^{D} d\varepsilon_4 \left\{ \frac{1}{\varepsilon_1 - \varepsilon_2} \frac{[1 - n_F(\varepsilon_1)]n_F(\varepsilon_3)}{\varepsilon_3 + \omega - \varepsilon_1} \frac{1}{\varepsilon_3 - \varepsilon_4} + (\varepsilon_1 \leftrightarrow \varepsilon_2) + (\varepsilon_3 \leftrightarrow \varepsilon_4) + (\varepsilon_1 \leftrightarrow \varepsilon_2 \text{ and } \varepsilon_3 \leftrightarrow \varepsilon_4) \right\}$$

$$\times \left\{ \frac{1}{a^6} \int_d^{\infty} dR_n R_n^2 \int_{r_0}^{d} dR_{n'} R_{n'}^2 [J_1(R_n, R_{n'}; k_1, k_2, k_3, k_4) + J_1(R_n, R_{n'}; k_3, k_4, k_1, k_2)] \right.$$

$$\left. + \frac{1}{a^6} \int_d^{\infty} dR_n R_n^2 \int_d^{\infty} dR_{n'} R_{n'}^2 J_2(R_n, R_{n'}; k_1, k_2, k_3, k_4) \right\}, \tag{7}$$

where r_0 is a short distance cutoff in the range of the atomic radius, and

$$J_1(R_n, R_{n'}; k_1, k_2, k_3, k_4) = (2\pi)^2 \int_{\theta_{n,\min}}^{\pi} d\theta_n \sin \theta_n \int_0^{\pi} d\theta_{n'} \sin \theta_{n'} F_2(R_n, R_{n'}, \theta_n, \theta_{n'}; k_1, k_2, k_3, k_4), \tag{8}$$

$$J_2(R_n, R_{n'}; k_1, k_2, k_3, k_4) = (2\pi)^2 \int_{\theta_{n,\min}}^{\pi} d\theta_n \sin \theta_n \int_{\theta_{n',\min}}^{\pi} d\theta_{n'} \sin \theta_{n'} F_2(R_n, R_{n'}, \theta_n, \theta_{n'}; k_1, k_2, k_3, k_4), \tag{9}$$

where $\theta_{n,\min} = \arccos(d/R_n)$ and $\theta_{n',\min} = \arccos(d/R_{n'})$.

Since, according to the earlier works,[2–4] the largest contribution comes from the first part of Eq. (7) corresponding to J_1, we will consider that.

The evaluation of the integrals with respect to θ_n and $\theta_{n'}$ gives

$$J_1(R_n,R_{n'};k_1,k_2,k_3,k_4) = \frac{4}{15}J^2\left(\frac{2\pi V^2\lambda}{\varepsilon_0^2}\right)^2\frac{d(R_n^2-d^2)}{R_n^3} \times [3v_0(k_2,R_n)v_1(k_1,R_n) + 3v_0(k_1,R_n)v_1(k_2,R_n) - 2v_1(k_1,R_n)v_1(k_2,R_n)$$

$$+ 2v_1(k_2,R_n)v_2(k_1,R_n) + 2v_1(k_1,R_n)v_2(k_2,R_n) - 8v_2(k_1,R_n)v_2(k_2,R_n)][3v_0(k_4,R_{n'})v_1(k_3,R_{n'})$$

$$+ 3v_0(k_3,R_{n'})v_1(k_4,R_{n'}) + v_1(k_3,R_{n'})v_1(k_4,R_{n'}) + 2v_1(k_4,R_{n'})v_2(k_3,R_{n'}) + 2v_1(k_3,R_{n'})v_2(k_4,R_{n'})$$

$$+ 4v_2(k_3,R_{n'})v_2(k_4,R_{n'})]. \tag{10}$$

Replacing k_1, k_2, k_3, and k_4 by k_F gives back the half of Eq. (B2) of Ref. 4.

After a straightforward calculation of the integrals with respect to R_n and $R_{n'}$ (see Appendix B), the first part of Eq. (7) corresponding to J_1 reads

$$\rho_0^4\int_{-D}^D d\varepsilon_1\int_{-D}^D d\varepsilon_2\int_{-D}^D d\varepsilon_3\int_{-D}^D d\varepsilon_4\left\{\frac{1}{\varepsilon_1-\varepsilon_2}\frac{[1-n_F(\varepsilon_1)]n_F(\varepsilon_3)}{\varepsilon_3+\omega-\varepsilon_1}\frac{1}{\varepsilon_3-\varepsilon_4}+(\varepsilon_1\leftrightarrow\varepsilon_2)+(\varepsilon_3\leftrightarrow\varepsilon_4)\right.$$

$$\left.+(\varepsilon_1\leftrightarrow\varepsilon_2 \text{ and } \varepsilon_3\leftrightarrow\varepsilon_4)\right\}\frac{4}{15}J^2\left(\frac{2\pi V^2\lambda}{\varepsilon_0^2}\right)^2[C(k_1d,k_2d)D(k_3d,k_4d)+C(k_3d,k_4d)D(k_1d,k_2d)], \tag{11}$$

where the functions C and D are given by Eqs. (B5) and (B11), respectively.

As C and D are symmetric in their variables, we can change the integration variables according to the changes indicated in the energy dependent factor in the integrand of Eq. (11), resulting in a simpler form like

$$\rho_0^4\int_0^D d\varepsilon_1\int_{-D}^D d\varepsilon_2\int_{-D}^0 d\varepsilon_3\int_{-D}^D d\varepsilon_4\left(\frac{1}{\varepsilon_1-\varepsilon_2}\frac{1}{\varepsilon_3+\omega-\varepsilon_1}\frac{1}{\varepsilon_3-\varepsilon_4}\right)4\frac{4}{15}J^2\left(\frac{2\pi V^2\lambda}{\varepsilon_0^2}\right)^2$$

$$\times[C(k_1d,k_2d)D(k_3d,k_4d)+C(k_3d,k_4d)D(k_1d,k_2d)], \tag{12}$$

where we have exploited the $1-n_F(\varepsilon_1)$ and $n_F(\varepsilon_3)$ factors as well.

III. THE ENERGY INTEGRALS

In the following, the asymptotic behavior for large distances d is considered; therefore, only the leading order in $1/d$ is kept everywhere.

For large distances, the radial electronic wave functions are fast oscillating as the energy is changed. These fast oscillations lead to essential cancellations. In order to keep track of the cancellations in the limit $d\to\infty$, the Riemann theorem with the first asymptotic correction is applied in the following forms:[12]

$$\int_a^b ds f(s)\cos(xs) \sim \frac{f(b)\sin(xb)}{x} - \frac{f(a)\sin(xa)}{x} \tag{13a}$$

and

$$\int_a^b ds f(s)\sin(xs) \sim \frac{f(a)\cos(xa)}{x} - \frac{f(b)\cos(xb)}{x}, \tag{13b}$$

which are valid in the leading order in $1/x$, where f must be integrable.

Let us consider the integrations with respect to the energies. In the first part of Eq. (12), the integral with respect to ε_2 is

$$\int_{-D}^D d\varepsilon_2\frac{C(k_1d,k_2d)}{\varepsilon_1-\varepsilon_2} = \int_{k_F-D/v_F}^{k_F+D/v_F} dk_2\frac{C(k_1d,k_2d)}{k_1-k_2}. \tag{14}$$

Introducing a new integration variable $\Delta k=k_2-k_1$ and using linear dispersion $\varepsilon=v_F(k-k_F)$, the integral reads

$$-\int_{-k_1+k_F-D/v_F}^{-k_1+k_F+D/v_F} d(\Delta k)\frac{C(k_1d,(k_1+\Delta k)d)}{\Delta k}$$

$$= -\frac{d^3}{a^3}\int_{-k_1+k_F-D/v_F}^{-k_1+k_F+D/v_F} d(\Delta k)\left(f_{c+}(k_1d,(k_1+\Delta k)d)\left[\cos(2k_1d)\frac{\cos(\Delta kd)}{\Delta k} - \sin(2k_1d)\frac{\sin(\Delta kd)}{\Delta k}\right]\right.$$

$$+ f_{c-}(k_1d,(k_1+\Delta k)d)\frac{\cos(\Delta kd)}{\Delta k} + f_{s+}(k_1d,(k_1+\Delta k)d)\left[\sin(2k_1d)\frac{\cos(\Delta kd)}{\Delta k} + \cos(2k_1d)\frac{\sin(\Delta kd)}{\Delta k}\right]$$

$$+ df_{s-}(k_1d,(k_1+\Delta k)d)\sin(\Delta kd) + \Delta kd^2f_{ci}(k_1d,(k_1+\Delta k)d)\{Ci[(2k_1+\Delta k)d] - Ci(\Delta kd)\}\right), \tag{15}$$

where we used the symmetry property of the cosine integral function $Ci(-x)=Ci(x)$ and trigonometrical identities.[13]

To evaluate the terms containing the $Ci(x)$ function we use

$$Ci(x) = -\int_x^\infty du \frac{\cos u}{u} = -\int_1^\infty dv \frac{\cos xv}{v} \tag{16}$$

and change the order of the integrations with respect to v and Δk.

Due to the cosine and sine functions in the integrand, the integral is determined by the singularity at $\Delta k = 0$ ($k_2 = k_1$). Searching for this singularity, we expand the f functions around $k_1 d$ in their second variables and then drop the terms which are not singular at $\Delta k = 0$. Then, the integral in Eq. (15) is

$$-\frac{d^3}{a^3}\int_{-k_1+k_F-D/v_F}^{-k_1+k_F+D/v_F} d(\Delta k) \left\{ \frac{\cos(\Delta k d)}{\Delta k}[f_{c+}(k_1 d, k_1 d)\cos(2k_1 d) + f_{c-}(k_1 d, k_1 d) + f_{s+}(k_1 d, k_1 d)\sin(2k_1 d)] \right.$$

$$\left. + \frac{\sin(\Delta k d)}{\Delta k}[-f_{c+}(k_1 d, k_1 d)\sin(2k_1 d) + f_{s+}(k_1 d, k_1 d)\cos(2k_1 d)] \right\}. \tag{17}$$

The range of the integrations can be extended to $-\infty \to \infty$ as those integrals are independent of d, while the added parts are fast oscillating and, therefore, they are $\mathcal{O}(1/k_F d)$, as can be proven by using the Riemann theorem given by Eq. (13). Then, using

$$\int_{-\infty}^\infty d(\Delta k) \frac{\cos(\Delta k d)}{\Delta k} = 0 \tag{18}$$

and

$$\int_{-\infty}^\infty d(\Delta k) \frac{\sin(\Delta k d)}{\Delta k} = \pi, \tag{19}$$

we get for Eq. (14)

$$\int_{-D}^D d\varepsilon_2 \frac{C(k_1 d, k_2 d)}{\varepsilon_1 - \varepsilon_2} = \frac{d^3}{a^3}\pi[f_{c+}(k_1 d, k_1 d)\sin(2k_1 d) - f_{s+}(k_1 d, k_1 d)\cos(2k_1 d)]$$

$$\approx \frac{d^3}{a^3}\pi\left[\frac{3825}{4(k_1 d)^6}\sin(2k_1 d) - \frac{225}{2(k_1 d)^5}\cos(2k_1 d)\right] \approx -\frac{d^3}{a^3}\frac{225\pi}{2(k_1 d)^5}\cos(2k_1 d), \tag{20}$$

where we kept only the leading order contribution in $1/k_1 d$ as $k_1 d \geq k_F d \gg 1$ according to the range of the integration with respect to k_1 (ε_1) in Eq. (12). Let us turn to the integration with respect to ε_1 in the first part of Eq. (12), i.e., to

$$\int_0^D \frac{d\varepsilon_1}{\varepsilon_3 + \omega - \varepsilon_1}\int_{-D}^D d\varepsilon_2 \frac{C(k_1 d, k_2 d)}{\varepsilon_1 - \varepsilon_2}$$

$$= -\frac{d^3}{a^3}\int_0^D \frac{d\varepsilon_1}{\varepsilon_3 + \omega - \varepsilon_1}\frac{225\pi}{(k_1 d)^5}\frac{1}{2}\cos(2k_1 d)$$

$$= -\frac{d^3}{a^3}\int_{k_F}^{k_F+D/v_F} \frac{dk_1}{k_3 + \frac{\omega}{v_F} - k_1}\frac{225\pi}{(k_1 d)^5}\frac{1}{2}\cos(2k_1 d). \tag{21}$$

As $\varepsilon_3 < 0$ ($k_3 < k_F$) in Eq. (12) and $\omega \approx 0$, the integrand has no singularities in the range of the integration; thus, in order to find the leading-order contribution in $1/k_F d$, we can apply the Riemann theorem given by Eq. (13). Then, Eq. (21) is

$$\int_0^D \frac{d\varepsilon_1}{\varepsilon_3 + \omega - \varepsilon_1}\int_{-D}^D d\varepsilon_2 \frac{C(k_1 d, k_2 d)}{\varepsilon_1 - \varepsilon_2}$$

$$\approx \frac{d^3}{a^3}\frac{v_F}{\varepsilon_3 + \omega}\frac{225\pi}{(k_F d)^5}\frac{1}{2}\frac{\sin(2k_F d)}{2d} = \frac{225\pi}{(k_F a)^3}\frac{\varepsilon_F}{\varepsilon_3 + \omega}\frac{1}{4}\frac{\sin(2k_F d)}{(k_F d)^3} \tag{22}$$

in leading order in $1/k_F d$, where we kept only the contribution of the lower limit, as the contribution of the upper limit of the integral in Eq. (22) is proportional to $1/D$; thus, it is of lower order.

Now we have to evaluate the remaining integrals with respect to ε_3 and ε_4 in the first part of Eq. (12) i.e.,

$$\int_{-D}^0 d\varepsilon_3 \frac{1}{\varepsilon_3 + \omega}\int_{-D}^D d\varepsilon_4 \frac{D(k_3 d, k_4 d)}{\varepsilon_3 - \varepsilon_4}. \tag{23}$$

Starting with the first part of Eq. (23) corresponding to the g functions in D [see Eq. (B11)], we again introduce a new integration variable $\Delta k = k_4 - k_3$ and use linear dispersion. Thus, Eq. (23) reads

$$\int_{k_F-D/v_F}^{k_F} dk_3 \frac{1}{k_3 - k_F + \dfrac{\omega}{v_F}} \int_{k_F-D/v_F}^{k_F+D/v_F} dk_4 \frac{D(k_3d,k_4d)}{k_3 - k_4} = -\int_{k_F-D/v_F}^{k_F} dk_3 \frac{1}{k_3 - k_F + \dfrac{\omega}{v_F}} \int_{-k_3+k_F-D/v_F}^{-k_3+k_F+D/v_F} d(\Delta k) \frac{D(k_3d,(k_3+\Delta k)d)}{\Delta k}. \quad (24)$$

In the first part containing the g functions [see Eq. (B11)], we can repeat the considerations used in performing the integrals with respect to ε_1 and ε_2, giving

$$\frac{d^3}{a^3}\pi\int_{k_F-D/v_F}^{k_F} dk_3 \frac{1}{k_3 - k_F + \dfrac{\omega}{v_F}}[g_{c+}(k_3d,k_3d)\sin(2k_3d)$$

$$- g_{s+}(k_3d,k_3d)\cos(2k_3d)]. \quad (25)$$

Since $k_F - D/v_F > 0$, we can again apply the Riemann theorem given by Eq. (13). The terms coming from the lower limit of the integrals are less by $1/D$ than the terms coming from the upper limit of the integral, which give

$$-\frac{d^3}{a^3}\pi\frac{v_F}{\omega}$$

$$\times\left[g_{c+}(k_Fd,k_Fd)\frac{\cos(2k_Fd)}{2d} + g_{s+}(k_Fd,k_Fd)\frac{\sin(2k_Fd)}{2d}\right]$$

$$\approx -\frac{d^3}{a^3}\pi\frac{v_F}{\omega}\left[\frac{225}{2(k_Fd)^4}\frac{\cos(2k_Fd)}{2d} - \frac{1125}{(k_Fd)^5}\frac{\sin(2k_Fd)}{2d}\right]$$

$$\approx -\frac{1}{(k_Fa)^3}\frac{\varepsilon_F}{\omega}\frac{225\pi}{4(k_Fd)^2}\cos(2k_Fd), \quad (26)$$

where only the leading-order contribution in $1/k_Fd$ was kept.

Turning to the second part of Eq. (23) corresponding to the h functions in D [see Eq. (B11)], after using the following properties:

$$h\left(k_3d,k_4d,\frac{r_0}{d}\right) = \frac{1}{(k_Fd)^3}h\left(\frac{k_3}{k_F},\frac{k_4}{k_F},k_Fr_0\right), \quad (27)$$

for the $h_{c+/c-/s+}$ functions [see Eq. (B13)] and

$$(k_3-k_4)dh_{s-}\left(k_3d,k_4d,\frac{r_0}{d}\right)$$

$$= \left(\frac{k_3}{k_F}-\frac{k_4}{k_F}\right)\frac{1}{(k_Fd)^3}h_{s-}\left(\frac{k_3}{k_F},\frac{k_4}{k_F},k_Fr_0\right) \quad (28)$$

for the h_{s-} function, and introducing the $s = k_3/k_F$ and $t = k_4/k_F$ new integration variables, we get

$$\frac{1}{(k_Fa)^3}\frac{P_1(k_Fr_0,\omega)}{15\pi}, \quad (29)$$

where

$$P_1(x,\omega) = 15\pi\int_{1-D/\varepsilon_F}^{1} ds \frac{1}{s-1+\dfrac{\omega}{\varepsilon_F}}\int_{1-D/\varepsilon_F}^{1+D/\varepsilon_F} dt \frac{H(s,t,x)}{s-t}$$

$$(30)$$

and

$$H(s,t,x) = h_{c+}(s,t,x)\cos[(s+t)x] + h_{c-}(s,t,x)\cos[(s-t)x]$$

$$+ h_{s+}(s,t,x)\sin[(s+t)x]$$

$$+ (s-t)h_{s-}(s,t,x)\sin[(s-t)x]. \quad (31)$$

Thus, the terms corresponding to the h functions give d-independent contribution; therefore, Eq. (23) is Eq. (29) in leading order in $1/k_Fd$.

Combining Eq. (29) with Eqs. (22) and (12), we get for the first part of Eq. (12) in leading order in $1/k_Fd$ the following:

$$16\varepsilon_F(J\rho_0)^2\frac{\Delta^2\lambda^2}{\epsilon_0^4}\frac{1}{(k_Fa)^6}P_1(k_Fr_0,\omega)\frac{\sin(2k_Fd)}{(k_Fd)^3}, \quad (32)$$

where $\Delta = \pi V^2\rho_0$ is the width of the d-levels due to hybridization.[10]

Turning to the second part of Eq. (12), after changing the integration variables as $\varepsilon_1 \leftrightarrow \varepsilon_3$ and $\varepsilon_2 \leftrightarrow \varepsilon_4$ and performing similar calculation as before, we get in leading order with respect to $1/k_Fd$ the following:

$$16\varepsilon_F(J\rho_0)^2\frac{\Delta^2\lambda^2}{\epsilon_0^4}\frac{1}{(k_Fa)^6}P_2(k_Fr_0,\omega)\frac{\sin(2k_Fd)}{(k_Fd)^3}, \quad (33)$$

where

$$P_2(x,\omega) = 15\pi\int_{1}^{1+D/\varepsilon_F} ds \frac{1}{s-1-\dfrac{\omega}{\varepsilon_F}}\int_{1-D/\varepsilon_F}^{1+D/\varepsilon_F} dt \frac{H(s,t,x)}{s-t}.$$

$$(34)$$

TABLE I. Comparison of $P^{num}(x,\omega=0.01)$ obtained by numerical integration and $P^{appr}(x,\omega=0)$ obtained by Eq. (37) for $x \sim 0.5 - 1.5$.

x	0.5	0.75	1	1.25	1.5
$P^{num}(x,\omega=0.01)$	−135.8	−428.1	−916.5	−1552.9	−2215.9
$P^{appr}(x,\omega=0)$	−138.3	−438.4	−952.6	−1664.6	−2514.1

Thus, the anisotropy factor coming from the first part of Eq. (7) corresponding to J_1—giving the leading contribution[2–4]—in leading order in $1/k_F d$ is

$$K = 16\varepsilon_F(J\rho_0)^2 \frac{\Delta^2\lambda^2}{\epsilon_0^4} \frac{1}{(k_F a)^6} P(k_F r_0, \omega) \frac{\sin(2k_F d)}{(k_F d)^3}, \quad (35)$$

where

$$P(x, \omega) = P_1(x, \omega) + P_2(x, \omega), \quad (36)$$

which is finite for $\omega=0$.

Evaluating P by numerical integration, it turns out that for $x \sim 1$,[14] the integrals with respect to t and s are dominated by the $t=s$ and $s=1$ singularities, respectively. Thus,

$$P(x, \omega = 0) \approx 15\pi \int_0^2 ds \frac{H(s,s,x)}{s-1} \ln \left| \frac{s}{s-2} \right|$$

$$= 15\pi H(1,1,x)\frac{\pi^2}{2}, \quad (37)$$

where we used $D=\varepsilon_F$. In Table I, we compare the results obtained by numerical integration and by Eq. (37) for $x \sim 0.5-1.5$.

The result of Eq. (35) for the anisotropy factor is essentially different from the earlier one [see Eq. (31) of Ref. 4] obtained by an unjustified assumption which corresponds formally to the approximations $C(k_1 d, k_2 d) \approx C(k_F d, k_F d)$ and $D(k_3 d, k_4 d) \approx D(k_F d, k_F d)$ in Eq. (12). The main differences are:

(1) It contains the oscillating factor $\sin(2k_F d)$.

(2) The asymptotic distance dependence is $1/(k_F d)^3$ instead of $1/k_F d$; thus, it is essentially weaker.

(3) Instead of the $f(\omega/D)P^{\text{old}}(k_F r_0)$ factor which contains the short-range cutoff r_0 and is estimated to be between 50 and 950 for $\omega \approx 0$ and $k_F r_0 \sim 0.5-1.5$, we have $P^{\text{new}}(k_F r_0, \omega)$ which is between -140 and -2500 for $\omega=0$ and $k_F r_0 \sim 0.5-1.5$; thus, in the asymptotic region using the same parameters as in Eq. (32) in Ref. 4,

$$\frac{0.01}{(d/\text{Å})^3} \text{ eV} < |K_d| < \frac{1.75}{(d/\text{Å})^3} \text{ eV}. \quad (38)$$

Finally, we can raise the question of how justified is the assumption of homogeneous distribution of the spin-orbit scatterers. In order to give the answer, in the following the scatterers are considered homogeneously distributed on sheets which are parallel to the surface and separated by a distance a. According to previous works,[3,4] the pair of sheets in equal distances from the impurity do not contribute to the anisotropy; thus, only the unpaired ones must be considered. The sheet n is in the distance na from the impurity and only sheets with $n>d/a$ are considered. As discussed in Refs. 2–4, one of the two scatterers n and n' is near the impurity and the other one is far from it on one of the sheets considered. Therefore, the contributions of the sheets are additive. The contributions of sheet n can be easily obtained from the present calculation as
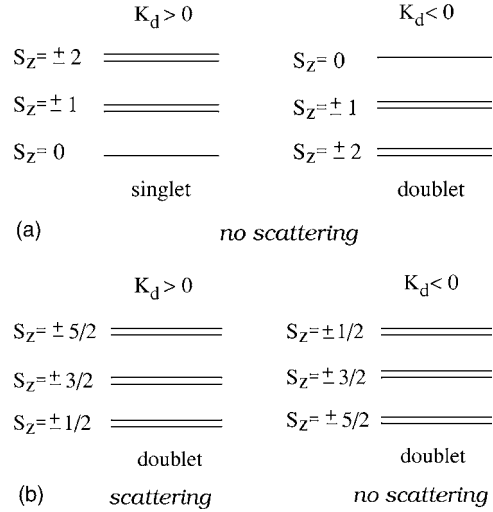

FIG. 3. The level splitting due to the surface anisotropy for (a) integer (e.g., $S=2$) and (b) half-integer (e.g., $S=5/2$) spins. It is also indicated whether the electrons can be scattered by the degenerate ground states or not.

$$K_n = a \frac{\partial}{\partial d} K_d \Big|_{d=na}, \quad (39)$$

where the derivative gives the contribution of an infinitely narrow layer and the prefactor provides the correct normalization. Thus, the final result in the asymptotic region is

$$K = \sum_{n>d/a}^{\infty} K_n \approx \sum_{n>d/a} 2ak_F \frac{\cos(2k_F na)}{(k_F na)^3}, \quad (40)$$

where the omitted prefactor is the same as in Eq. (35).

Thus, the separate sheets contribute by different signs and amplitudes. Due to the fast decay by increasing n, only sheets of restricted numbers are essential. Adding the contribution of the sheets with different signs and amplitudes (likely randomly distributed), the final amplitude of the anisotropy $|K|$ can be larger than $|K_d|$; thus, the $1/d^3$ decay rate can be somewhat reduced. The situation is different in a coherent case with $k_F a = p\pi$, where p is an integer. For even p, the contributions have the same sign and $\sum_{n>d/a} 1/n^3 \sim a^2/d^2$, which provides a slower decay rate.

IV. CONCLUSIONS

The amplitude of the anisotropy is oscillating and weaker than the one earlier estimated.[3,4] In these changes, the sharp edge in the R integral and thus, the existence of the surface are crucial. We used a uniform distribution of the spin-orbit scatterers in space. Considering the question of how the results are changed in the case where continuum layers of the scatterers are considered, it is argued that the overall behavior is not expected to change, but that only the amplitude can be influenced moderately. Furthermore, it is assumed that the spin-orbit scattering is pointlike, but a finite extension r_d (it is assumed that $k_F r_d < \pi$) smears somewhat the $\sin(2k_F d)$ function in Eq. (35). The actual size of that can be estimated only by electronic structure calculations and certainly will be

included in the recent work of one of the authors (Szunyogh) and his co-workers, which is in progress.[9]

How the spin is frozen by the surface anisotropy is essentially different from how it is done in the previous works[3,4] as K_d is not always positive (see Fig. 3) and also depends on whether the spin is integer or half-integer.

(i) *Integer spin* (*e.g.*, $S=2$). The ground state is either a singlet or a doublet depending on the sign of K_d; however, the electron cannot be scattered by transition in the doublet as the spin momentum difference is $\Delta S = \pm 4$ and turning the electron spin allows only $\Delta S = \pm 1$. Thus, the spin at low temperature can be completely frozen in.

(ii) *Half-integer spin* (*e.g.*, $S=5/2$). The ground state is always a doublet; however, in one of the cases $\Delta S = \pm 1$ which can cause scattering, in contrast to the case where $\Delta S = \pm 5$. Thus, only half of the impurities can cause electron spin flips at low temperature, which is different from the previously assumed $K_d > 0$ case.

This result shows analogies with Ref. 15, where magnetic molecules with large spins on a metallic surface were considered. The spin levels are split in a similar way and electron induced transitions are allowed only between certain levels.

For comparison with experiment, the preasymptotic behavior is very essential, which is beyond the scope of the present paper. The electronic calculations in progress[9] must provide this information including the amplitude of the anisotropy as in the other model in Ref. 8.

The present results valid in the asymptotic region can provide a good possibility of testing the numerical calculation. Detailed comparison with experiments will follow after the completion of the numerical calculation, which will provide more necessary information.

APPENDIX A:

The $v_m(k)$ matrix elements are the same as in Eq. (13) of Ref. 4:

$$v_0(k,R_n) = 10\left[\frac{\sin(kR_n)}{2kR_n} + \frac{3\cos(kR_n)}{(kR_n)^2} - \frac{12\sin(kR_n)}{(kR_n)^3} - \frac{27\cos(kR_n)}{(kR_n)^4} + \frac{27\sin(kR_n)}{(kR_n)^5}\right],$$

$$\text{(A1a)}$$

$$v_1(k,R_n) = 15\left[-\frac{\cos(kR_n)}{(kR_n)^2} + \frac{5\sin(kR_n)}{(kR_n)^3} + \frac{12\cos(kR_n)}{(kR_n)^4} - \frac{12\sin(kR_n)}{(kR_n)^5}\right],$$

$$\text{(A1b)}$$

$$v_2(k,R_n) = 15\left[-\frac{\sin(kR_n)}{(kR_n)^3} - \frac{3\cos(kR_n)}{(kR_n)^4} + \frac{3\sin(kR_n)}{(kR_n)^5}\right].$$

$$\text{(A1c)}$$

The F_1 and F_2 functions are defined in the same way as in Ref. 4, namely,

$$F_1(R_n,\theta_n,R_{n'},\theta_{n'};k_1,k_2,k_3,k_4) = \frac{2J^2}{\epsilon_0^4}f_{1122} \quad \text{(A2a)}$$

and

$$F_2(R_n,\theta_n,R_{n'},\theta_{n'};k_1,k_2,k_3,k_4) = \frac{2J^2}{\epsilon_0^4}(f_{1111} - f_{1212} - f_{1122}),$$

$$\text{(A2b)}$$

where

$$f_{\sigma_1\sigma_2\sigma_3\sigma_4} = \sum_{\substack{mm' \\ \sigma_1\sigma_2}} \widetilde{W}_{m_1m_2}^{k_1k_2}(R_n,\theta_n)\widetilde{W}_{m_2m_1}^{k_4k_3}(R_{n'},\theta_{n'}). \quad \text{(A3)}$$

$\widetilde{W}$ gives the form of W in the rotated coordinate system (where the z axis is perpendicular to the surface) given by

$$\widetilde{W}_{kk'}_{\substack{mm' \\ \sigma\sigma'}}(R_n,\theta_n) = \delta_{m+\sigma,m'+\sigma'}\sum_{\substack{\bar{m}\bar{m}' \\ \bar{\sigma}\bar{\sigma}'}} d_{m\bar{m}}^{(2)}(\theta_n)d_{\sigma\bar{\sigma}}^{(1/2)}$$

$$\times(\theta_n)W_{kk'}_{\substack{\bar{m}\bar{m}' \\ \bar{\sigma}\bar{\sigma}'}}(R_n)d_{\bar{m}'m'}^{(2)}(-\theta_n)d_{\bar{\sigma}'\sigma'}^{(1/2)}(-\theta_n),$$

$$\text{(A4)}$$

where the Wigner formula for rotation matrices[16] was used.

APPENDIX B:

Here, we perform the integrations with respect to R_n and $R_{n'}$ in the first part of Eq. (11). Let us start with the integration with respect to R_n, namely,

$$\widetilde{C}(k_1,k_2) := \frac{1}{a^3}\int_d^\infty dR_n R_n^2 \frac{d(R_n^2 - d^2)}{R_n^3}[3v_0(k_2,R_n)v_1(k_1,R_n)$$

$$+ 3v_0(k_1,R_n)v_1(k_2,R_n) - 2v_1(k_1,R_n)v_1(k_2,R_n)$$

$$+ 2v_1(k_2,R_n)v_2(k_1,R_n) + 2v_1(k_1,R_n)v_2(k_2,R_n)$$

$$- 8v_2(k_1,R_n)v_2(k_2,R_n)]. \quad \text{(B1)}$$

After substituting the $v_m(k,R_n)$ matrix elements given by Eq. (A1) and introducing the dimensionless integration variable $y = R_n/d$ and notations $t_1 = k_1d$ and $t_2 = k_2d$, we get

$$\widetilde{C}(k_1,k_2) = C(k_1d,k_2d), \quad \text{(B2)}$$

where

$$C(t_1,t_2) = \frac{d^3}{a^3} \int_1^\infty dy \frac{y^2-1}{y} \{C_{c+}(t_1,t_2,y)\cos[(t_1+t_2)y]$$

$$+ C_{c-}(t_1,t_2,y)\cos[(t_1-t_2)y]$$

$$+ C_{s+}(t_1,t_2,y)\sin[(t_1+t_2)y]$$

$$+ C_{s-}(t_1,t_2,y)\sin[(t_1-t_2)y]\}. \tag{B3}$$

The occurring integrals with respect to y look like

$$G_c(t,n) := \int_1^\infty dy \frac{y^2-1}{y} \frac{\cos(ty)}{y^n} \tag{B4a}$$

and

$$G_s(t,n) := \int_1^\infty dy \frac{y^2-1}{y} \frac{\sin(ty)}{y^n}. \tag{B4b}$$

Evaluating the G_s and G_c functions analytically by using MATHEMATICA, we get

$$C(t_1,t_2) = \frac{d^3}{a^3} \{f_{c+}(t_1,t_2)\cos(t_1+t_2) + f_{c-}(t_1,t_2)\cos(t_1-t_2)$$

$$+ f_{s+}(t_1,t_2)\sin(t_1+t_2) + (t_1-t_2)f_{s-}(t_1,t_2)\sin(t_1-t_2)$$

$$+ (t_1-t_2)^2 f_{ci}(t_1,t_2)[\text{Ci}(t_1+t_2) - \text{Ci}(t_1-t_2)]\}, \tag{B5}$$

where for $t_1=t_2=t \gg 1$,

$$f_{c+}(t,t) \approx \frac{3825}{4t^6},$$

$$f_{c-}(t,t) \approx -\frac{225}{2t^4},$$

$$f_{s+}(t,t) \approx \frac{225}{2t^5},$$

$$f_{s-}(t,t) \approx \frac{225}{2t^4},$$

$$f_{ci}(t,t) \approx \frac{225}{2t^4}, \tag{B6}$$

and $\text{Ci}(t) = -\int_t^\infty du(\cos u/u)$ is the cosine integral function.

Let us consider now the integration with respect to $R_{n'}$ in the first part of Eq. (11):

$$\tilde{D}(k_3,k_4) := \frac{1}{a^3} \int_{r_0}^d dR_{n'} R_{n'}^2 [3v_0(k_4,R_{n'})v_1(k_3,R_{n'})$$

$$+ 3v_0(k_3,R_{n'})v_1(k_4,R_{n'}) + v_1(k_3,R_{n'})v_1(k_4,R_{n'})$$

$$+ 2v_1(k_4,R_{n'})v_2(k_3,R_{n'}) + 2v_1(k_3,R_{n'})v_2(k_4,R_{n'})$$

$$+ 4v_2(k_3,R_{n'})v_2(k_4,R_{n'})]. \tag{B7}$$

After substituting the $v_m(k,R_{n'})$ matrix elements given by Eq. (A1) and introducing the dimensionless integration variable $y'=R_{n'}/d$ and notations $t_3=k_3 d$, $t_4=k_4 d$, and $y_0=r_0/d$, we get

$$\tilde{D}(k_3,k_4) = D(k_3 d, k_4 d), \tag{B8}$$

where

$$D(t_3,t_4) = \frac{d^3}{a^3} \int_{y_0}^1 dy' y'^2 \{D_{c+}(t_3,t_4,y')\cos[(t_3+t_4)y']$$

$$+ D_{c-}(t_3,t_4,y')\cos[(t_3-t_4)y']$$

$$+ D_{s+}(t_3,t_4,y')\sin[(t_3+t_4)y']$$

$$+ D_{s-}(t_3,t_4,y')\sin[(t_3-t_4)y']\}. \tag{B9}$$

The occurring integrals with respect to y' look like

$$H_c(t,n) := \int_{y_0}^1 dy' y'^2 \frac{\cos(ty')}{y'^n} \tag{B10a}$$

and

$$H_s(t,n) := \int_{y_0}^1 dy' y'^2 \frac{\sin(ty')}{y'^n}. \tag{B10b}$$

Evaluating the H_s and H_c functions analytically by using MATHEMATICA, we get

$$D(t_3,t_4) = \frac{d^3}{a^3} \{g_{c+}(t_3,t_4)\cos(t_3+t_4) + g_{c-}(t_3,t_4)\cos(t_3-t_4)$$

$$+ g_{s+}(t_3,t_4)\sin(t_3+t_4) + (t_3-t_4)g_{s-}(t_3,t_4)\sin(t_3-t_4)$$

$$+ h_{c+}(t_3,t_4,y_0)\cos[(t_3+t_4)y_0]$$

$$+ h_{c-}(t_3,t_4,y_0)\cos[(t_3-t_4)y_0]$$

$$+ h_{s+}(t_3,t_4,y_0)\sin[(t_3+t_4)y_0]$$

$$+ (t_3-t_4)h_{s-}(t_3,t_4,y_0)\sin[(t_3-t_4)y_0]\}, \tag{B11}$$

where for $t_3=t_4=t \gg 1$,

$$g_{c+}(t,t) \approx \frac{225}{2t^4},$$

$$g_{c-}(t,t) \approx \frac{225}{2t^4},$$

$$g_{s+}(t,t) \approx -\frac{1125}{t^5},$$

$$g_{s-}(t,t) \approx \frac{1125}{2t^6}, \tag{B12}$$

and

$$h_{c+}(t_3,t_4,y_0) = \frac{20\,250}{t_3^5 t_4^5 y_0^7} - \frac{8100}{t_3^3 t_4^5 y_0^5} - \frac{20\,250}{t_3^4 t_4^4 y_0^5} - \frac{8100}{t_3^5 t_4^3 y_0^5} + \frac{1350}{t_3^2 t_4^4 y_0^3}$$
$$+ \frac{6525}{2 t_3^3 t_4^3 y_0^3} + \frac{1350}{t_3^4 t_4^2 y_0^3} - \frac{225}{2 t_3^2 t_4^2 y_0}, \tag{B13a}$$

$$h_{c-}(t_3,t_4,y_0) = -\frac{20\,250}{t_3^5 t_4^5 y_0^7} + \frac{8100}{t_3^3 t_4^5 y_0^5} - \frac{20\,250}{t_3^4 t_4^4 y_0^5} + \frac{8100}{t_3^5 t_4^3 y_0^5} + \frac{1350}{t_3^2 t_4^4 y_0^3}$$
$$- \frac{6525}{2 t_3^3 t_4^3 y_0^3} + \frac{1350}{t_3^4 t_4^2 y_0^3} - \frac{225}{2 t_3^2 t_4^2 y_0}, \tag{B13b}$$

$$h_{s+}(t_3,t_4,y_0) = \frac{20\,250}{t_3^4 t_4^5 y_0^6} + \frac{20\,250}{t_3^5 t_4^4 y_0^6} - \frac{1350}{t_3^2 t_4^5 y_0^4} - \frac{8100}{t_3^3 t_4^4 y_0^4} - \frac{8100}{t_3^4 t_4^3 y_0^4}$$
$$- \frac{1350}{t_3^5 t_4^2 y_0^4} + \frac{1125}{2 t_3^3 t_4^3 y_0^2} + \frac{1125}{2 t_3^2 t_4^2 y_0^2}, \tag{B13c}$$

and

$$h_{s-}(t_3,t_4,y_0) = -\frac{20\,250}{t_3^5 t_4^5 y_0^6} + \frac{1350}{t_3^3 t_4^5 y_0^4} - \frac{6750}{t_3^4 t_4^4 y_0^4} + \frac{1350}{t_3^5 t_4^3 y_0^4} - \frac{1125}{2 t_3^3 t_4^3 y_0^2}. \tag{B13d}$$

[1] See, e.g., M. A. Blachly and N. Giordano, Phys. Rev. B **51**, 12537 (1995); G. Neuttiens, J. Eom, C. Strunk, V. Chandrasekhar, C. Van Haesendonck, and Y. Bruynseraede, Europhys. Lett. **34**, 617 (1996); N. Giordano, Phys. Rev. B **53**, 2487 (1996); C. Strunk, M. Henny, C. Schonenberger, G. Neuttiens, and C. Van Haesendonck, Phys. Rev. Lett. **81**, 2982 (1998); T. M. Jacobs and N. Giordano, Phys. Rev. B **62**, 14145 (2000); E. Seynaeve, K. Temst, F. Aliev, C. Van Haesendonck, V. N. Gladilin, V. M. Fomin, and J. T. Devreese, Phys. Rev. Lett. **85**, 2593 (2000), further references can be found in Ref. 2.

[2] O. Újsághy and A. Zawadowski, J. Phys. Soc. Jpn. **74**, 80 (2005).

[3] O. Újsághy, A. Zawadowski, and B. L. Gyorffy, Phys. Rev. Lett. **76**, 2378 (1996).

[4] O. Újsághy and A. Zawadowski, Phys. Rev. B **57**, 11598 (1998).

[5] V. M. Fomin, V. N. Gladilin, J. T. Devreese, C. Van Haesendonck, and G. Neuttiens, Solid State Commun. **106**, 293 (1998).

[6] J. Friedel, Nuovo Cimento, Suppl. **7**, 287 (1958).

[7] L. Szunyogh and B. L. Gyorffy, Phys. Rev. Lett. **78**, 3765 (1997).

[8] L. Szunyogh, G. Zaránd, S. Gallego, M. C. Muñoz, and B. L. Gyorffy Phys. Rev. Lett. **96**, 067204 (2006).

[9] A. Szilva, L. Szunyogh, G. Zaránd, and M. C. Muñoz (unpublished).

[10] P. W. Anderson, Phys. Rev. **124**, 41 (1961).

[11] A. A. Abrikosov, Physics (Long Island City, N.Y.) **2**, 5 (1965).

[12] The formula can be proved by integration by part.

[13] M. Abramowitz and I. Stegun, *Handbook of Mathematical Functions* (Dover, New York, 1972).

[14] For $x \gg 1$, the approximate expression [Eq. (37)] is not valid: for, e.g., $x = 10$ we get $P^{num}(x = 10, \omega = 0.01) = 8992.5$ while $P^{appr}(x = 10, \omega = 0) = -1297.3$.

[15] C. Romeike, M. R. Wegewijs, W. Hofstetter, and H. Schoeller, Phys. Rev. Lett. **96**, 196601 (2006).

[16] D. M. Brink and G. R. Satchler, *Angular Momentum* (Oxford University Press, Oxford, 1962).